Available online at www.sciencedirect.com
ScienceDirect
Journal of Power Sources 182 (2008) 441–448
JOURNAL OF POWER SOURCES
www.elsevier.com/locate/jpowsour

Design of an 80 kWe PEM fuel cell system: Scale up effect investigation

C. Bonnet [a,*], S. Didierjean [b], N. Guillet [c], S. Besse [d], T. Colinart [b], P. Carré [a]

[a] *Laboratoire des Sciences du Génie Chimique, Nancy-University-CNRS, 1 rue Grandville, BP20451, 54001 Nancy, France*
[b] *Laboratoire d'Energétique et de Mécanique Théorique et Appliquée, Nancy-University-CNRS, 2 avenue de la Forêt de Haye, 54504 Vandoeuvre les Nancy, France*
[c] *CEA-Grenoble LITEN/DTH/LCPEM, 17, rue des martyrs, 38054 Grenoble Cedex 9, France*
[d] *Hélion, Domaine du Petit Arbois, Bâtiment Jules Verne, BP71, 13545 Aix en Provence Cedex 4, France*

Received 31 October 2007; received in revised form 19 December 2007; accepted 19 December 2007
Available online 6 January 2008

Abstract

In the frame of SPACT-80 project to design and manufacture a robust and durable air/hydrogen 80 kWe PEM fuel cell for transportation application, experiments have been carried out on various electrode active surfaces since the full scale system could be damaged by some particular operating conditions. Thus, the main objective of this paper was to verify that a 25 cm^2 single cell, a 5-cell pilot stack and a 90-cell stack exhibit the same behaviour and that they are representative of the full device's performance. After a brief description of the studied device the scaling up effect was checked. In non-optimal conditions, experiments were mainly conducted on single cell and pilot stack. In driving cycle and when studying various gas flows, they present similar evolution for the cell voltage as well as for the water management. The water transport coefficient and the diffusion resistance values determined by impedance spectroscopy highlight the presence of liquid water that could have an effect on the gas transport to the electrode. Investigation on the air humidification conditions shows that at lower relative humidity (RH), the two fuel cells have similar behaviour but above 60% RH different evolutions appear. Whatever the air humidification conditions, liquid water is present in both compartments.
© 2008 Elsevier B.V. All rights reserved.

Keywords: PEM fuel cell; Scaling effect; Durability; Water management; Impedance spectroscopy

1. Introduction

The challenge in the future for automotive industry will be to develop even cleaner and more efficient vehicles in order to reduce or eliminate emissions of toxic gases and carbon dioxide, and to limit oil dependence. Batteries used in current hybrid gasoline-electric vehicles and full electric vehicles contribute to these objectives. However, energy storage is one problem facing electrical vehicles with weight and recharging duration which limits the driving range of traditional systems such as batteries. Fuel cell systems appear to be a very promising solution to overcome some of these limitations by using hydrogen as a fuel.

Proton exchange membrane fuel cells (PEMFC) have many advantages such as low operating temperature, high power density and good dynamic performance. These features make PEMFC the most promising and attractive candidate for transportation applications [1,2]. However, fuel cell cost and lifetime are the two most important challenges for wide use in transportation. Fuel cell electrocatalysts are still a major cost factor, due to their precious metal content. Current technological progresses on catalysts are expected to drastically reduce the price of the systems within the next years [3]. Automotive fuel cell systems will be required to be as durable and reliable as current automotive engines, i.e. 5000 h. The performance of current systems decreases substantially after ~1000 h. Thus, it is necessary to identify degradation mechanisms of the fuel cell components in operative conditions to minimize their effects and to reach performance specifications.

Since 2005, a consortium including CNRS laboratories (French National Centre for Scientific Research), CEA laboratories (National Atomic Research Centre), INRETS (National Institute for Research on Transportation and Safety), and FCLab (Fuel Cell Academic Research Lab) have taken part in the ANR-funded SPACT80 project with HELION (AREVA subsidiary), to design and manufacture a robust and durable air/H_2 80 kWe PEM fuel cell-based system, specifically developed

* Corresponding author. Tel.: +33 383 175 119; fax: +33 383 322 975.
E-mail address: caroline.bonnet@ensic.inpl-nancy.fr (C. Bonnet).

0378-7753/$ – see front matter © 2008 Elsevier B.V. All rights reserved.
doi:10.1016/j.jpowsour.2007.12.100

Nomenclature

F	Faraday constant (96,487 A s eq^{-1})
I	cell current (A)
$\dot{m}$	molar flow (mol s^{-1})
P	power (W cm^{-2})
R	specific resistance (Ω cm^2)
RH	relative humidity
Z	impedance (Ω)

Greek letters

α	water transport coefficient
λ_i	stoichiometric ratio of reacting species i

Subscripts

a	anode
c	cathode
ct	charge transfer
CPE	constant phase element
diff	diffusion
nom	nominal
w	water
Ω	ohmic

Exponents

out	outlet

for transportation applications [4,5]. Two end-users are also involved: SNCF (French National Railway Company) and the DGA (French Government Military Agency). The device has been designed to be tested on the hybrid locomotive demonstrator "LHyDIE" and on the four-wheel-drive hybrid demonstrator truck "ECCE" (Fig. 1). HELION, the project leader, supplies all the fuel cells and fuel cell stacks tested in the different laboratories and collaborates in the scientific developments. Scientific developments are aimed at improving the durability and the reliability of fuel cell systems in transport-like utilization.

All experiments required for completion of the program could not be carried out with the full scale system since the membrane electrode assembly (MEA) of the cells could be damaged by some particular operating conditions in the tests. A test procedure plan was prepared to decrease the electrodes active surface for the sake of cost reduction – for both investment and operating costs – allowing more experiments to be carried out. Thus, the main objective of this paper was to check that a 25 cm^2 single cell and a 340 cm^2/5-cell pilot stack have the same behaviour and are representative of the full device's 800 cm^2/90-cell stack performance. The first part of the paper gives a brief description of the studied device. Then we present the analysis of the experimental results obtained from various operating conditions conducted in 25 cm^2 single cells and 340 cm^2/5-cell pilot stacks.

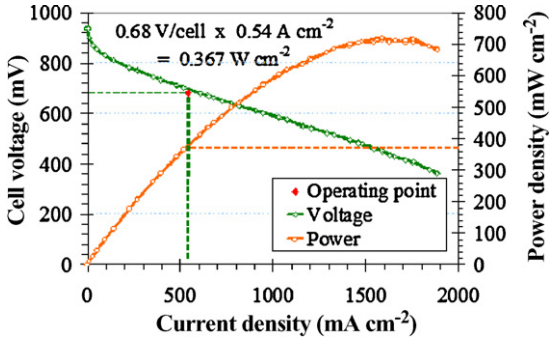

Fig. 2. Polarization curve obtained on a cell at operative conditions (70 °C; $P = 1.6 \times 10^5$ Pa; $\lambda_{H_2/air} = 1.2/2$; % $RH_{H_2/air} = 0/70\%$).

2. System specifications

System architecture was defined in agreement with technical requirements of the two testing platforms, representative of railway and automotive applications.

Specifications were to produce of a hydrogen/air PEM fuel cell system delivering more than 80 kWe for a railway application (460–620 V) and yielding up to 40% efficiency (based on H_2 LHV). Main components of the fuel cell such as membrane electrodes assemblies and gas diffusion layer were selected among several suppliers and qualified in order to reach 0.68 V per cell at a 0.54 A cm^{-2} current density. The design of bipolar plates was carefully studied to optimize the performance, in particular at low gas supply. An example of the fuel cell performance is given by the polarization curve shown in Fig. 2. At the nominal operating point ($P_{nom} = 0.367$ W cm^{-2}), the 25 cm^2 single cell, the 340 cm^2/5-cell pilot stack and the 800 cm^2/90 cell stack would deliver 9 W, 600 W and 30 kW, respectively.

Fig. 1. Demonstrators used to perform real application experiments for the SPACT-80 project.

Table 1
Technical specifications of the fuel cell-based system

Electric output	>80 kW (voltage = 540–750 V)
Dynamic	Maximum change rate, 200 A s^{-1}
System efficiency	>40%
Lifetime	>5000 h
Hydrogen	1.6×10^5 Pa; $\lambda = 1.2$ (recirculation)
Air	1.6×10^5 Pa; $\lambda = 2$
Temperature	343 K
Humidification	Air humidified at 70% RH
Weight/size	<1000 kg/3.1 m^3 (stack only)

The working temperature was regulated around 70 °C. Reactants gas pressure was set to 1.6×10^5 Pa and flows were regulated to feed the fuel cell with stoichiometric coefficients of 1.2/2 respectively for dry H_2 and 70% RH humidified air. The technical specifications of the fuel cell-based system are summarized in Table 1.

3. Experimental section

Experiments were conducted in conditions that may be unsafe for fuel cell durability. Therefore pilot stacks and 25 cm^2 single cells were chosen as samples for the experiments. Cumulated operation time over the fuel cell systems exceeded 27,000 h over the last 18 months period. Only typical results are presented and discussed here. Emphasis has been put on the scaling effect by verifying that the 25 cm^2 single cells and pilot stacks behaviour were representative of the full device's performance, and then by studying the effect of both air/hydrogen flows and gas humidification with 25 cm^2 single cells and 340 cm^2/5-cell pilot stacks.

3.1. Scaling effect on polarization curves and cycling

The polarization curves are plotted for the three samples studied: 25 cm^2 single cells, 5-cell pilot stacks and 90-cell stack. As reported in Fig. 3, the polarization curves are the same for the three different scales, representing four orders of magnitude on the device power.

Experiments were performed for 1000 h under constant current and following a driving cycle representative of a real railway

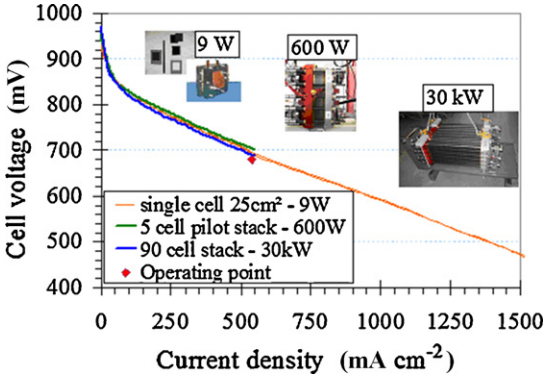

Fig. 3. Polarization curves obtained on the various tested devices: single cell, 5-cell pilot stack and 90-cell stack.

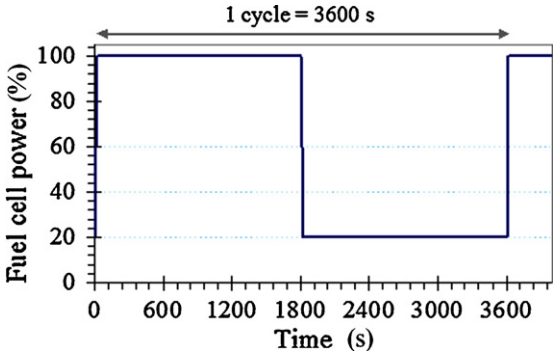

Fig. 4. Driving cycle applied to the system.

service suggested by INRETS (Fig. 4). The driving cycle considers hybridization of the electrical sources. Starting from a value at 20% of the nominal operating power (P_{nom} = 367 mW cm^{-2}), the power increases to reach the nominal power (100% P_{nom}) within 20 s. The power is stabilized for 30 min, and then it returns for 30 min to the initial value (20% P_{nom}).

Fig. 5 presents the profiles of the polarization curves obtained on the single cell and on a pilot stack induced by 550 h of operation under the driving cycle. The effect of the driving cycle is similar on the two fuel cells: for the nominal current density, the cell voltage was reduced by approximately 60 mV corresponding to an 8% loss of energy produced. Results obtained on the scale models can therefore be considered as representative of the full device's behaviour.

Further experiments were performed on three devices of different sizes. However experiments with "extreme" or hazardous conditions for the fuel cell durability were conducted on single cell and pilot stack. Consequently, the effect of gas flows and their humidification were investigated using the two smaller devices as presented below.

3.2. Effect of air/hydrogen flows on single cell and pilot stack

The cell temperature and pressure were fixed at 70 °C and 1.6×10^5 Pa. Hydrogen was kept dry whereas before entering the fuel cell, air was humidified to attain 70% relative humidity (operating conditions given in Table 1). For single cell,

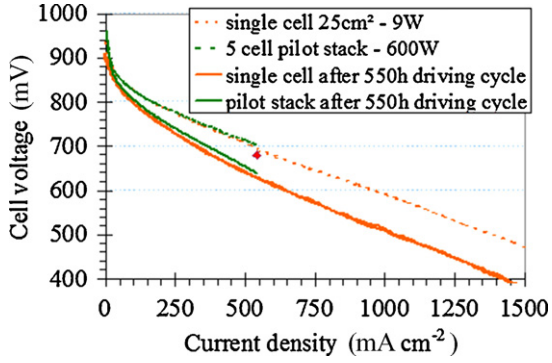

Fig. 5. Comparison of the polarization curves obtained on single cell and 5-cell pilot stack before and after 550 h of driving cycle aging.

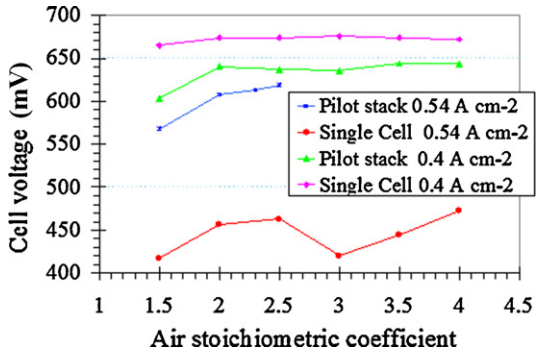

Fig. 6. Air flow effect on cell voltage with single cell and pilot stack at 0.54 and 0.4 A cm^{-2} ($\lambda_{H_2} = 1.2$).

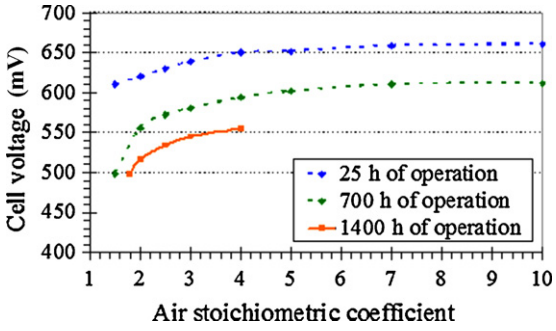

Fig. 8. Long duration tests on single cell at 0.8 A cm^{-2}.

the humidification was ensured in home-made packed columns filled with deionised water. The humidification temperature was imposed by a water bath for the heating of the humidifier. For pilot stack humidification is realized by over heated water vapour injection in the air stream. Experiments were conducted in galvanostatic mode, and the cell was fed with various reactant gas flows. Stoichiometric coefficient for air was varied from 1.5 to 4 while hydrogen's one was kept constant at 1.2. In a second series of experiments the stoichiometric coefficient of hydrogen was varied from 1.2 to 3 while that for air was kept constant at 2. Experiments were performed at two different current densities: 0.540 or 0.4 A cm^{-2}. For both single cells and pilot stacks the cell voltage was recorded for long time periods at constant reactants gas flows and current density, allowing steady-state behaviour to be attained, and water mass balances to be established. Impedance spectroscopy measurements were carried out on single cell at the considered gas flows and current density. Measurements were carried out using an Autolab PGSTAT302 (EcoChemie) potentiostat/galvanostat connected to an electronic load Kikusui PLZ664WA. Amplitude of the sine perturbation was fixed at 10% of the steady current (0.054 A cm^{-2}) for sufficient accuracy of the low frequency part of the spectra. Frequencies were scanned from 10 kHz to 100 mHz, with 10 points per decade.

Figs. 6 and 7 present the cell voltage variation with the stoichiometric factor of the two gases, for the single cell and pilot stack when changing the air or hydrogen flow. Experimental

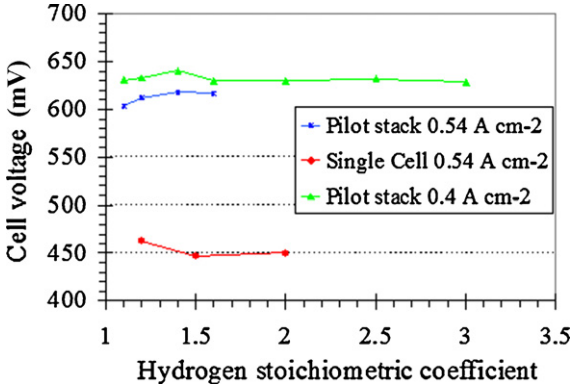

Fig. 7. Hydrogen flow effect on cell voltage with single cell and pilot stack at 0.54 and 0.4 A cm^{-2} ($\lambda_{air} = 2$).

results showed similar behaviours for the two devices, in spite of their sizes. Concerning the effect air flow, the cell voltage appears to be only slightly affected by a stoichiometric factor below 2. This result demonstrates the possibility to operate at low air supply during dynamic actions and also for several minutes in case of air supplier malfunction, flooding or leakage in the air feed line. For stoichiometric factor superior to 2, the cell voltage is not affected by this factor whatever the studied device and the current density. However, working at high stoichiometric factor is to result in severe drying of the membrane or, on the contrary could favour the water draining and limit the significance of the flooding phenomena. Concerning the hydrogen flow effect, for both single cells and pilot stack tests, no influence of gas flow variations on cell voltages was observed even at high stoichiometric coefficient.

Besides, long duration tests carried out at 0.8 A cm^{-2} with the single cell under the driving cycle showed a significant reduction in the electric performance depending on the stoichiometric factor value (Fig. 8). Along experiment time the fuel cell is more and more sensitive to the stoichiometric factor decrease under cycling.

The comparison of the results obtained for the influence of air flow on single cell at 0.54 A cm^{-2} (Fig. 6) and at 0.8 A cm^{-2} (Fig. 8, 25 h of operation) shows a larger impact of the stoichiometry on the cell voltage at 0.8 A cm^{-2} than at the lower current densities: at higher current density the system appears to be more sensitive to the gas transport limitation.

As explained above for the fuel cell systems single cell and pilot stack, once the cell voltage recorded, the amount of water leaving the two compartments of the cell, $\dot{m}^{out}_{w,a}$ and $\dot{m}^{out}_{w,c}$, were deduced from the amount of the liquid water collected, and taking into account the vapour pressure at the gas outlet temperature, which ranged from 25 to 30 °C for the single cell, and was equal to 5 ± 0.1 °C for the pilot stack. These measurements allowed water mass balances to be established. Also the water transport coefficient, α, defined as the ratio of the water transported to the anode over the flow of produced water through oxygen reduction could be thereafter calculated. Considering Faraday's law for oxygen reduction, and that hydrogen enters dry at the anode side, α was calculated as

$$\alpha = \frac{\dot{m}^{out}_{w,a}}{I/(2F)} \quad (1)$$

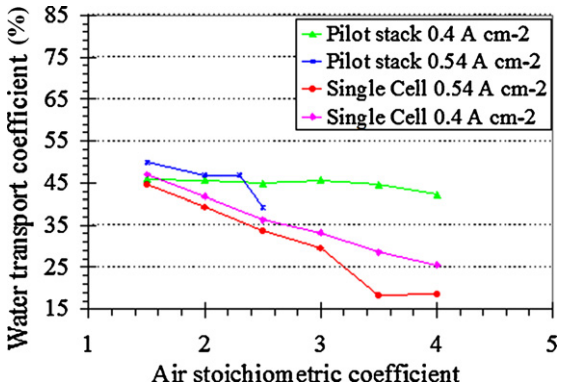

Fig. 9. Water management vs. the air stoichiometric coefficient.

Figs. 9 and 10 present the water transport coefficient (α) versus the stoichiometric factors of the reacting gases. Considering Fig. 9, whatever the sample size and current density, the amount of water transported from the cathode to the anode side is rather similar for the two fuel cell systems and decreases when the stoichiometric air factor increased. As a matter of fact, the larger the air flow is, the more important the amount of water at the cathode side is drained off. As expected, an increase in the hydrogen flow at the anode favours the transport of water through the membrane from the cathode side by diffusion (Fig. 10). Büchi and Srinivasan [6] obtained a similar result since the water removed from the anode, at a constant air stoichiometry, is a linear function of the hydrogen stoichiometry.

Figs. 9 and 10 show a large influence of the reactant gas flows on the amount of water collected at the anode side. The average relative humidity of the gas streams leaving the cell compartments and the liquid water fraction present at each compartment calculated from the weighing water collected, are presented in Figs. 11–14.

Whatever conditions, the gas issued from the anode side is always saturated with water, as shown by Büchi and Srinivasan [6]. The very large amount of liquid water can be explained by the low hydrogen flow at the outlet. Not the entire anode chamber but several areas could be flooded. Even if the kinetics is very fast at the anode, this could generate diffusion trouble. We can suppose that the bottom part of the anode is flooded and that the diffusion from the cathode to the anode is favoured at

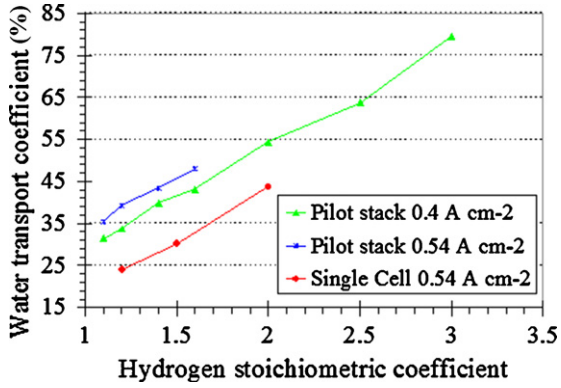

Fig. 10. Water management vs. the hydrogen stoichiometric coefficient.

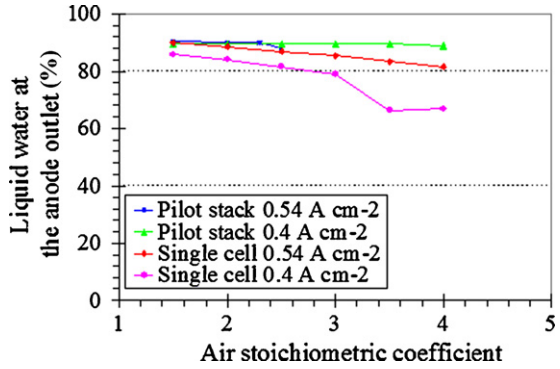

Fig. 11. Humidification conditions for the gas at the anode outlet depending on air flows.

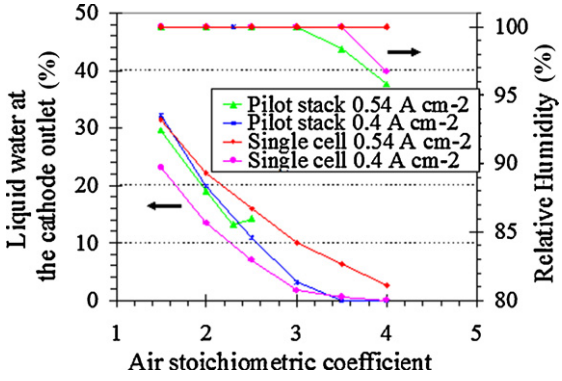

Fig. 12. Humidification conditions for the gas at the cathode outlet depending on air flows.

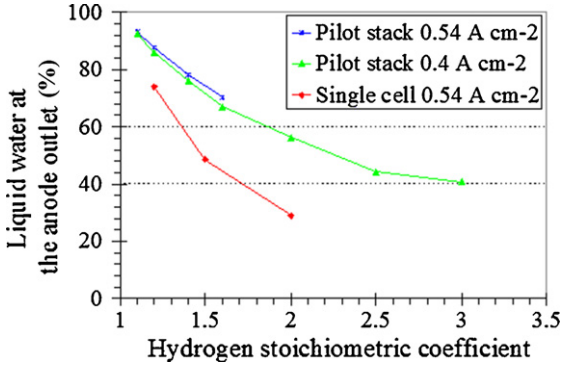

Fig. 13. Humidification conditions for the gas at the anode outlet depending on hydrogen flows.

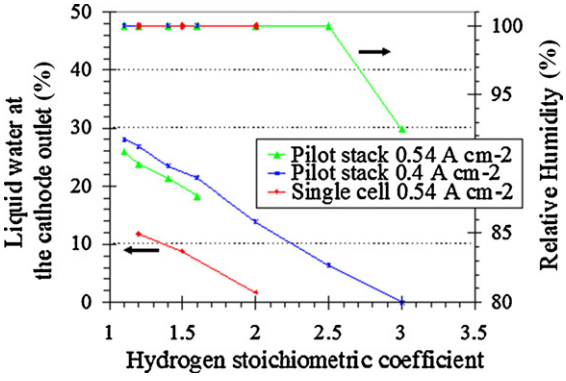

Fig. 14. Humidification conditions for the gas at the cathode outlet depending on hydrogen flows.

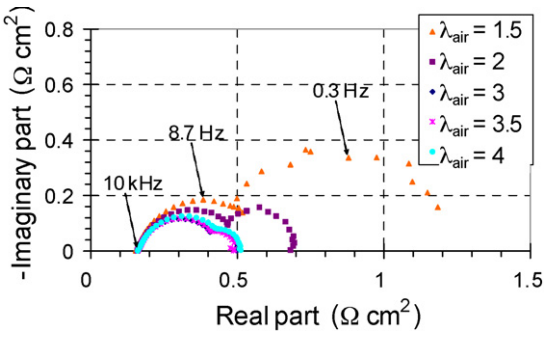

Fig. 15. Impedance spectra at 0.54 A cm^{-2} in single cell.

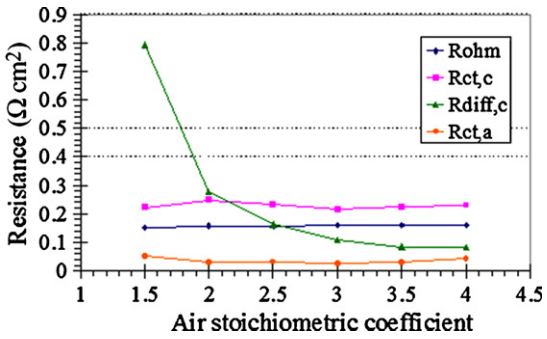

Fig. 17. Fitted values of the impedance spectra (Fig. 15) using the equivalent circuit.

the top part. A 2D-modelling could help us to better understand these transport phenomena. At the cathode, liquid water is often present in the outlet gas. For the other cases, the relative humidity was calculated at the cell temperature. For both fuel cell size and current density, it can be observed that the air flow rate increase causes a slight decrease of the amount of liquid water at the anode side which is to correlate to the significant decrease of the fraction of liquid water at the cathode chamber, as presented by Santarelli et al. [7] in a PEMFC stack. In the same way, increasing hydrogen flow leads to a larger flux of gas at the anode outlet. Consequently a larger flow of water vapour can thereafter be removed from the anode side which means lower amount of water liquid. A larger transport of water through the membrane from the cathode to the anode side and so a decrease of liquid water at the cathode is allowed.

The large amount of liquid water could have an impact on diffusion transport of the species in the cell structure. Thus, more accurate analysis was achieved by impedance spectroscopy, as shown in Fig. 15 at 0.54 A cm^{-2} in single cell when changing the air flow.

Spectra present three more or less distinct loops, referred as high, medium and low frequency loops. The high frequency loop could correspond to the hydrogen oxidation [8]. The medium frequency loop, on the left part, is usually attributed to the cathode charge transfer resistance. The low frequency loop is described as corresponding to diffusion of species like oxygen through nitrogen or the backing layer [9,10], or water through the active layer or the membrane [11,12].

The impedance model was established using the equivalent circuit technique as shown in Fig. 16. Charge transfer resistances are set in parallel with the double-layer capacitance: in

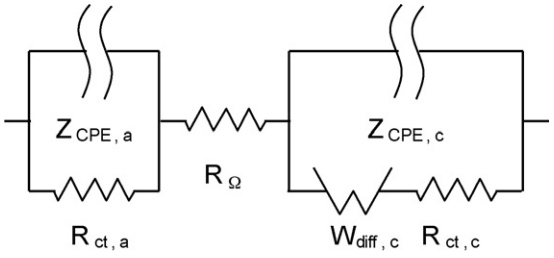

Fig. 16. Electrical equivalent circuit for impedance spectra. R_Ω: ohmic resistance, R_{ct}: charge transfer resistance, Z_{CPE}: constant phase element, W: diffusion-convection Warburg element.

fact, a constant phase element (CPE) was used instead of pure capacitances in the equivalent circuit. The high frequency loop corresponds to the left part of the circuit, and the medium/low frequency loops correspond to the right part. Fitting the spectra to the model impedance yields estimation of the charge transfer resistance at the anode and cathode sides, the ohmic resistance and the diffusion resistance at the cathode. This last one is related to the Warburg impedance. At the anode this resistance is generally neglected.

Fig. 17 presents the resistance values deduced from the fitting. Only the diffusion resistance is affected by the air flow; with a regular decreasing variation when the flow increases. From a stoichiometric factor equal to 3.5, the resistance attains a steady level with the air flow. This result is consistent with the hydration conditions (Fig. 12). According to which the higher fraction of liquid water was observed at low stoichiometric factor values. Thus, the gas transport to the electrode is more difficult, resulting in higher diffusion resistance. Conversely reducing the amount of liquid water facilitates the gas transport, then leading to lower diffusion resistance.

3.3. *Effect of air humidification on single cell and pilot stack*

The operating conditions are given in Table 1. The fuel cell temperature was fixed at 70 °C and was running under 1.6×10^5 Pa. Stoichiometric coefficients for air and hydrogen were kept constant at 2 and 1.2, respectively, and relative humidity of air was varied from 10 to 100%. As for experiments above, the cell voltage of the two fuel cells was recorded for long-term periods, and water mass balances were established under steady-state conditions.

Fig. 18 presents the air humidification effect on the cell voltage with the single cell and the pilot stack. In spite of noticeable differences, the cell voltage usually increased with the inlet RH below 60%. Beyond this value, the variations seem to depend on the cell: whereas the voltage of the single cell still increased with RH, the voltage of small stack at 0.54 A cm^{-2} decreased with higher relative humidity. For lower current density, RH seems to be of little influence on the stack voltage.

Fig. 19 shows a large influence of the air humidification on the amount of water collected at the anode side. For both fuel cells, water transport coefficient increases with relative humidity

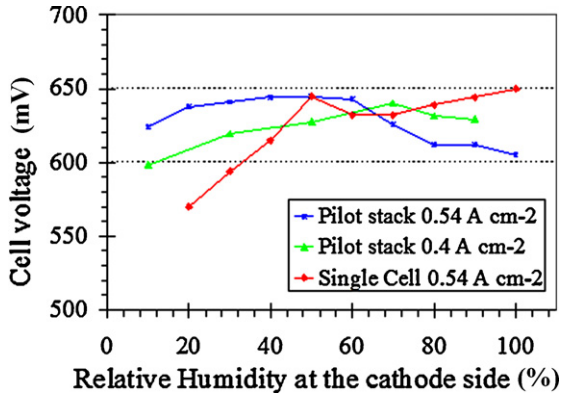

Fig. 18. Air humidification effect on cell voltage with single cell and pilot stack at 0.54 and 0.4 A cm^{-2}.

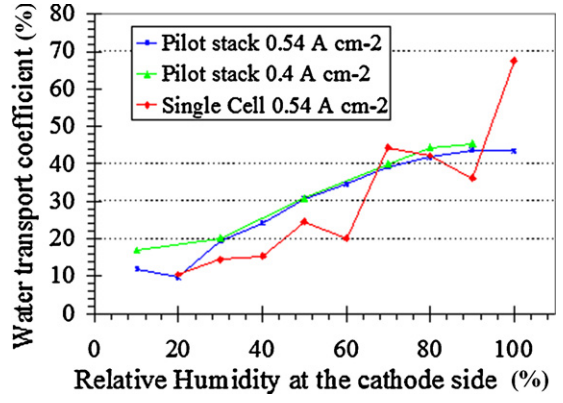

Fig. 19. Water management as a function of air humidification.

at the cathode side, corresponding to higher water flux to the anode side by diffusion. The average relative humidity of the gas streams leaving the cell compartments and the liquid water fraction calculated by mass balances from experimental data, are presented in Figs. 20 and 21.

Obviously, the higher the air humidification is, the larger the amount of water inside the cell. This favours the transport of water to the anode side and the presence of liquid water at both compartments, as presented in Figs. 19–21. These results are in agreement with the work of Cai et al. [13] who showed that when a thin membrane was used in a cell the flooding degree

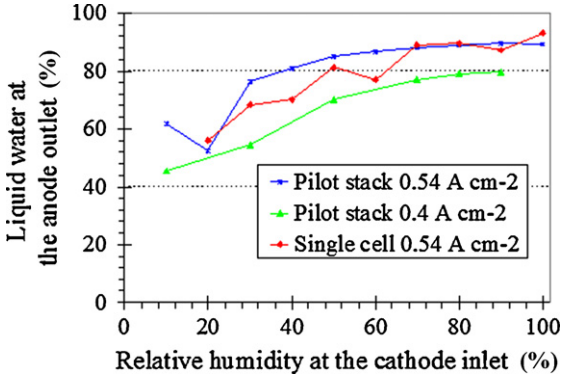

Fig. 20. Humidification conditions for the gas at the anode outlet depending on air humidification.

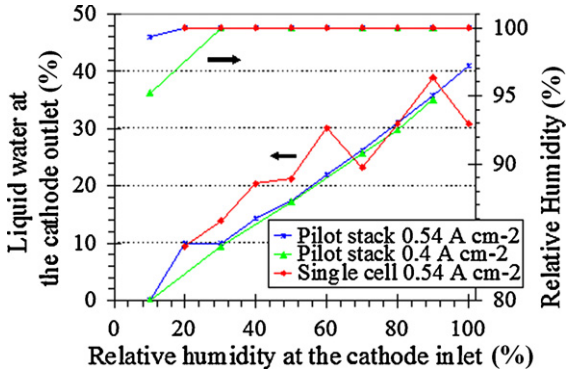

Fig. 21. Humidification conditions for the gas at the cathode outlet depending on air humidification.

in the cathode and the anode was increased while the cathode humidity increased.

A minimum of gas hydration is needed for better performance. However an over humidification can lead to the cell flooding since the water condensation will limit the gas feed of the active sites [14].

4. Conclusion

In the objective of SPACT-80 project to design and manufacture a robust and durable air/hydrogen 80 kWe PEM fuel cell for transportation application, experiments have been carried out on various electrode active surfaces (25 cm^2 single cell, 340 cm^2/5-cell pilot stack and 800 cm^2/90-cell stack). To our knowledge, there are very few studies on the scale effect presented in the literature [15]. In a first part, the scaling effect was verified since the polarization curves are the same for the three different scales. In non-optimal conditions, experiments were mainly conducted on single cell and pilot stack. In driving cycle, 25 cm^2 single cell and 340 cm^2/5-cell pilot stack present similar evolution.

The study on the effect of air/hydrogen flows on single cell and pilot stack shows similar behaviour for the two sizes. The cell voltage is not significantly affected by the gas flows. Nevertheless, the water management is largely dependent on the reactant gas flows. The gas streams leaving the cell were shown to be over a wide area saturated with water with a large part of liquid water that could have an effect on the gas transport to the electrode. This result was verified by the diffusion resistance values determined by impedance spectroscopy. In this way, it seems to be better to work at air stoichiometric factor around 2.5. A higher coefficient does not seem sensible since the compressor characteristics could be changed. At the anode side, a hydrogen stoichiometric factor around 1.2 could be applied, this means to work in recirculation. However other problems could appear as the increase of nitrogen concentration in hydrogen flow because of the cross-over through the membrane and as the presence of water in the hydrogen flow inlet.

The study of the effect of air humidification is not exactly conclusive since at lower relative humidity, the two fuel cells have similar behaviour but above 60% RH different evolutions appear. Whatever the air humidification conditions, liquid water

is present at both the compartments. The amount of liquid water increases with higher humidification.

For all the experiments done, liquid water is present at the anode and the cathode sides. With time this could accelerate the materials degradation and thus the electric performance of the fuel cell. Experiments performed on single cells and pilot stacks let us to define the best operating conditions yielding to the highest performance and the lowest degradation on the complete 80 kWe system.

Acknowledgement

This work was supported by the French government through the "Agence Nationale de la Recherche—Pan'H" hydrogen program.

References

[1] S. Gottesfeld, T. Zawodzinski, Adv. Electrochem. Sci. Eng. 5 (1997) 195–301.
[2] G.J.K. Acres, J.C. Frost, G.A. Hards, R.J. Potter, T.R. Ralph, D. Thompsett, G.T. Burstein, G.J. Hutchings, Catal. Today 38 (1997) 393–400.
[3] G.J. Suppes, Int. J. Hydrogen Energy 31 (3) (2006) 353–360.
[4] N. Guillet, S. Didierjean, A. Chenu, C. Bonnet, P. Carré, B. Wahdame, F. Harel, D. Hissel, S. Besse, S. Boblet, V. Chaudron, A. De Bernardinis, G. Coquery, S. Escribano, N. Bardi, International Electric Vehicle Symposium and Exposition, Anaheim, CA, USA, 2007.
[5] D. Candusso, F. Harel, A. De Bernardinis, X. François, M.-C. Péra, D. Hissel, P. Schott, G. Coquery, J.-M. Kaufmann, Int. J. Hydrogen Energy 31 (2006) 1019–1030.
[6] F.N. Büchi, S. Srinivasan, J. Electrochem. Soc. 144 (8) (1997) 2767–2772.
[7] M.G. Santarelli, M.F. Torchio, M. Cali, V. Giaretto, Int. J. Hydrogen Energy 32 (2007) 710–716.
[8] M. Boillot, C. Bonnet, N. Jatroudakis, P. Carre, S. Didierjean, F. Lapicque, Fuel Cells 1 (2006) 31–37.
[9] T.J.P. Freire, E.R. Gonzalez, J. Electroanal. Chem. 503 (2001) 57–68.
[10] T.E. Springer, T.A. Zawodzinski, M.S. Wilson, S. Gottesfeld, J. Electrochem. Soc. 143 (1996) 587–599.
[11] N. Wagner, W. Schnurnberger, B. Müller, M. Lang, Electrochim. Acta 43 (1998) 3785–3793.
[12] V.A. Paganin, C.L.F. Oliveira, E.A. Ticianelli, T.E. Springer, E.R. Gonzalez, Electrochim. Acta 43 (1998) 3761–3766.
[13] Y. Cai, J. Hu, H. Ma, B. Yi, H. Zhang, Electrochim. Acta 51 (2006) 6361–6366.
[14] S. Shimpalee, U. Beuscher, J.W. Van Zee, Electrochim. Acta 52 (2007) 6748–6754.
[15] D. Chu, R. Jiang, J. Power Sources 80 (1999) 226–234.